

# The Simulation of the SLS Process as the Basis of a Process Optimization

J. Steinberger, J. Shen, K. Manetsberger, J. Muellers\*

DaimlerChrysler Research Center  
Ulm, Germany

\*DaimlerChrysler Research, Dornier GmbH  
Friedrichshafen, Germany

## Abstract

In this work, a new model of the SLS process is introduced, offering the chance of analytically optimizing Selective Laser Sintering. The laser energy input is calculated by considering multiple scattering in the powder bed. The heat transfer is described by a new model which considers the heat flow through the growing sintering neck, and the sintering dynamics are determined by a new viscoelastic sintering model. All theoretical models are verified through experiments at near SLS conditions and are implemented in an enhanced FEM simulation of the process. Through this simulation, the major problems of the Selective Laser Sintering are illustrated and approaches for optimization of the SLS process are shown.

## Introduction

Since Rapid Prototyping is becoming better known and more widely accepted in the industrial goods industry, the growth of a number of new fields of application has accompanied this trend. But as a result, the demand for improved accuracy and enhanced mechanical properties of the prototype parts has also increased steadily. Especially in the aerospace industry with its high standards are the requirements set for the variety of RP technologies extremely demanding. Hence, a major concern must be to integrate Rapid Prototyping investment casting parts in flyable plane prototypes.

In the Rapid Prototyping investment casting process, conventional wax models are replaced by RP polymer models. The premasters can be manufactured using any of a number of RP technologies. A study by DaimlerChrysler, however, shows that Selective Laser Sintering has the greatest potential to fulfill the tolerance class requirements set by the European aerospace industry (2/3 A<sub>2</sub>, VDG P690). Thus, the basic requirement is optimization of both the material and the process itself. In the past, attempts to solve the major problem incurred in the SLS process - the inhomogeneous temperature distribution in the part and in the powder bed - were more empirical than analytical. This uneven temperature distribution is the result of the local energy input in the powder bed, which leads to an inhomogeneous sinter density and consistency and to tension and distortion.

The purpose of the work was to develop a process simulation to optimize the SLS process and to control it intelligently. The basis for this is a detailed, SLS process-relevant description of the single physical processes. To achieve this, Selective Laser Sintering is separated into the four physical processes set out below /NEL93/, /NÖK96/:

- Propagation of electromagnetic waves which stem from the laser and the thermal radiation.
- Heat transfer within the powder bed.
- Powder sintering due to thermal absorption of the laser power.
- Post-sintering process.

These four single processes are experimentally explored, modeled and implemented in an FEM simulation which enables the major problems of the Selective Laser Sintering of polymers to be analyzed and concepts for optimization of the process to be provided.

### Propagation of the Electromagnetic Waves

Both the local energy input and the local conversion of radiation energy into heat are responsible for the form and the energy distribution of the emerging volume heat source, which are all strongly affected by the propagation of the laser beam in the powder bed. In their description of the SLS process, Sun /SUN91/ and Keller /KEL99/ use strongly simplified models for the propagation of the laser energy. Sun assumes that the radiation is absorbed within the first layer of particles. Keller, however, supposed that the intensity of the radiation is reduced exponentially with a characteristic effective penetration depth  $D_{p\_eff}$ . This penetration depth is inversely proportional to the solid fraction of the powder sample:

$$D_{p\_eff} = \frac{D_{p\_solid}}{\exp}$$

In the Sun model, the penetration depth is strongly dependent on the particle size, whereas it is totally independent in the Keller model. They both neglect multiple scattering, which leads to incorrect results, especially when the particle size and the laser wavelength are in the same dimensions /PEL93/. Neither Sun nor Keller verified their theory in relevant experiments.

In this work, the propagation of the laser beam in the powder bed is calculated, taking multiple scattering into account. Here, the scattering by a single particle is considered using the Mie theory. The transfer onto the powder bed is done using the radiative transfer theory ([1]), which is commonly employed in astrophysics. This approximate solution considers multiple scattering but neglects the interference of the scattered rays. This simplification can be used, since the powders utilized in the SLS process are characterized by a great statistical disorder /ISH78/. /KOK99/. Equation [1] is solved by means of Monte-Carlo simulation.

$$\frac{d\vec{I}(\vec{r}, \vec{\omega})}{dz} = N C_{ext} \vec{I}(\vec{r}, \vec{\omega}) + \int_{4\pi} \vec{I}(\vec{r}, \vec{\omega}', \vec{\omega}) N C_{str}^{diff}(\vec{\omega}', \vec{\omega}) d\vec{\omega}' + B_0(\vec{r}, \vec{\omega}), \quad [1]$$

$$C_{sca} = \int_{4\pi} C_{str}^{diff}(\vec{\omega}, \vec{\omega}') d\vec{\omega}'$$

where  $\vec{I}(\vec{r}, \vec{\omega})$  is the intensity vector at  $\vec{r}$  with the direction of  $\vec{\omega}$ ,  $C_{ext}$ ,  $C_{str}$  is the extinction or scattering cross section,  $N$  is the concentration of the particles in the observed layer  $dz$  and  $B_0(\vec{r}, \vec{\omega})$  is the source.

The validity of the transport theory in the case of the SLS process has been proved in transmission experiments (*Figure 1*), where a CO<sub>2</sub> laser beam is focused on a thin and well-defined layer of PMMA and PA-12 powder. The transmitted radiation is measured integrally by means of an Ulbricht scope and differentially by aperture. This means that both the decrease in the intensity and the divergence of the ray could be measured. *Figure 2* shows the excellent consistence between the transport theory and experiment.

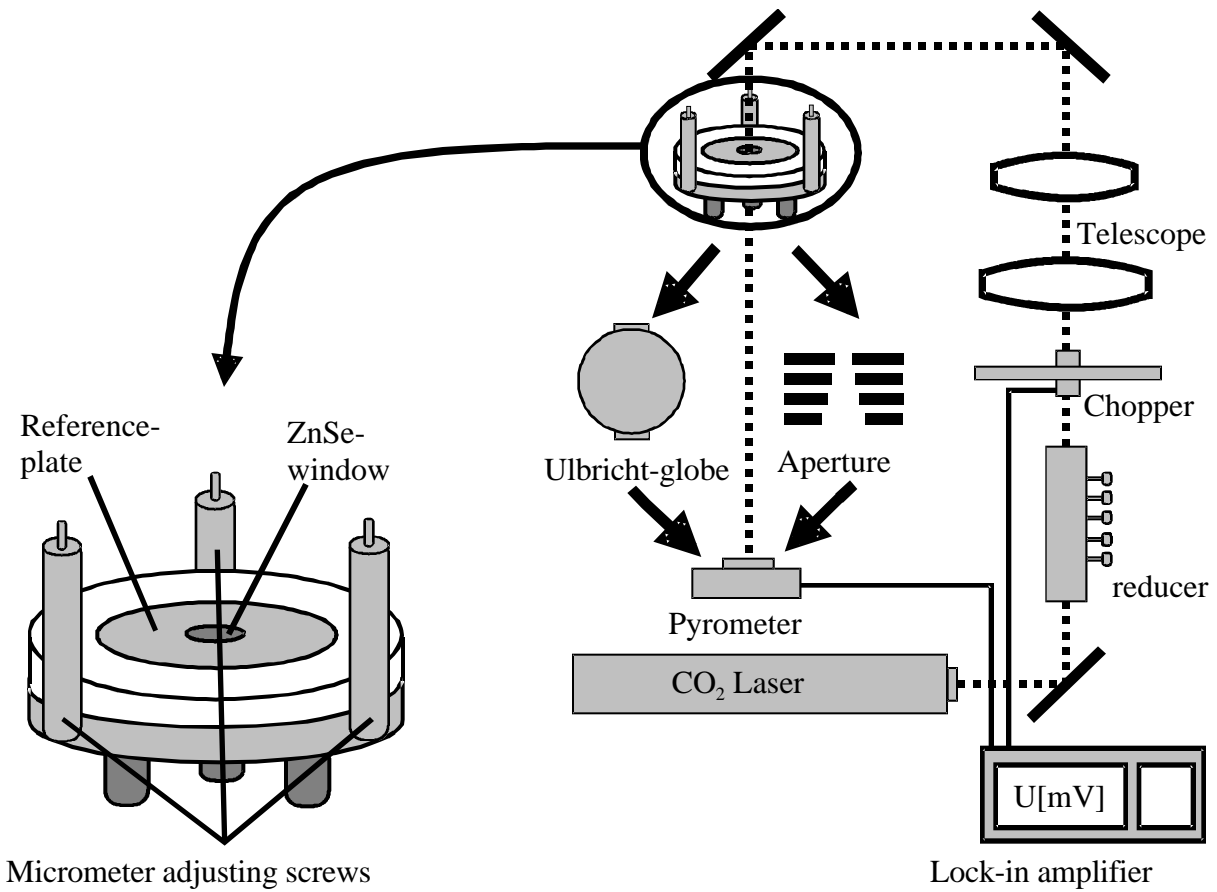


Figure 1: Transmission experiment

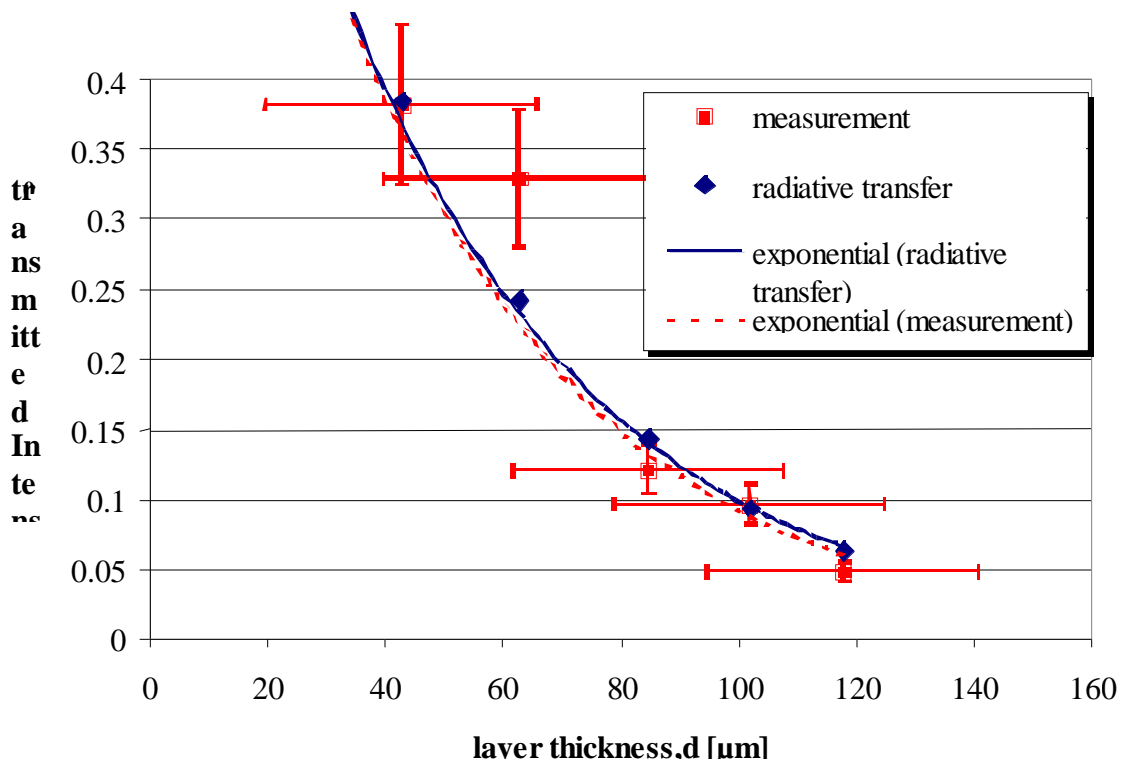
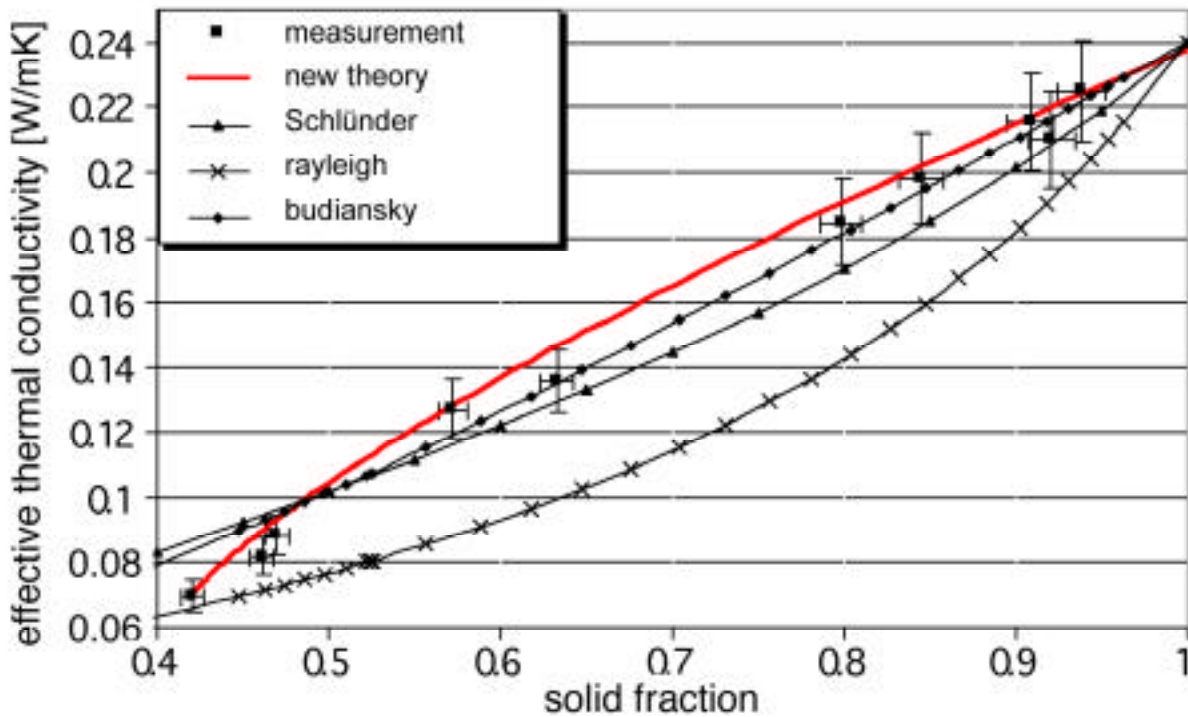


Figure 2: Comparison of transmission experiment and transport theory

## Heat Transfer

The heat transfer in a statistically distributed powder can only be determined after a number of simplifications have been performed. In existing models, a unit cell in which the heat transfer is calculated alternatively for the powder /SCH88/ is formulated. The difference between the particle geometry and the ideal spherical geometry is considered using an empirical form factor. In the case of Selective Laser Sintering, however, the geometry of the sintered particle changes steadily during the process. Due to the transformation of the laser energy into heat, a sintering neck between the particles is formed. It describes a thermal bridge that grows with the sintering time. These dynamical geometrical changes cannot be considered in existing models. *Figure 3* shows insufficient consistency between various existing models and the experiment.



*Figure 3: Heat transport:- comparison of theory and experiment*

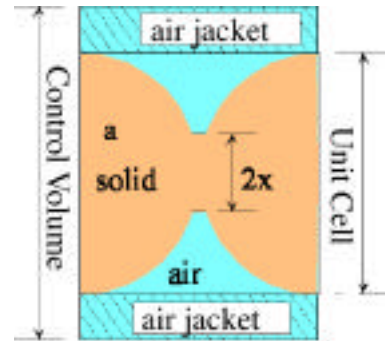
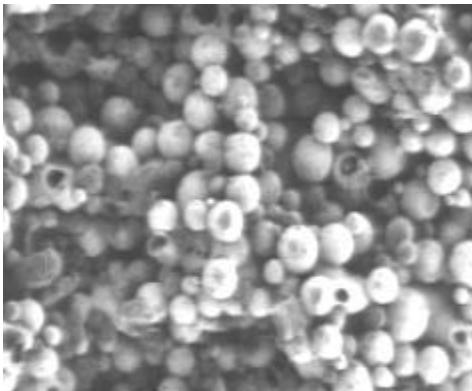


*Figure 4: Unit cell for the calculation of the heat transfer*

Thus, we present a new model which takes the formation of a sintering neck into account. Similar to existing models, a unit cell is created. The central issue of the unit cell is the change of the sintering neck (Figure 4).

The thermal conductivity in the unit cell as a function of the sintering neck  $x/a$  can be calculated as follows:

$$E = \frac{x^2}{a^2} + \frac{2}{3} \left( 1 - \frac{x^2}{a^2} \right)^{\frac{3}{2}}. \quad [2]$$

The discrepancy between the geometrically calculated solid fraction in the unit cell and the experimentally determined solid fraction is leveled through an air jacket [STE99]. This allows the solid fraction to be calculated as a function of the sintering neck:

$$\frac{x}{a} = \frac{x^2}{a^2} + \frac{2}{3} \left( 1 - \frac{x^2}{a^2} \right)^{\frac{3}{2}} \left( 1 - \frac{1 - \frac{x^2}{a^2} - \frac{2}{3} \left( 1 - \frac{x^2}{a^2} \right)^{\frac{3}{2}}}{1 - \frac{1 - \frac{x^2}{a^2} - \frac{2}{3} \left( 1 - \frac{x^2}{a^2} \right)^{\frac{3}{2}}}{\frac{1}{3}}} \right). \quad [3]$$

where  $\epsilon_{\text{exp}}$  is the experimentally determined solid fraction. The thermal radiation is described under consideration of multiple scattering. Figure 3 emphasizes that only the new model shows sufficient consistency of theory and experimental data.

### Sintering Dynamics

The sintering dynamics affect both the propagation of the laser radiation and the thermal heat diffusion because of corresponding changes of the powder bed porosity [Sch88], [THI83], [NEL93]. Since an understanding of sintering is essential to be able to model the SLS process, a fair amount of theoretical and experimental work has been reported on this subject. In earlier papers, the sintering rate kinetics used to simulate SLS processing was determined from isothermal, unidirectional powder densification studies carried out in oven experiments. The time scales of the experiments were several orders of magnitude larger than the time scales of the SLS process. Therefore, Steinberger et al. have presented an experiment that determined the sintering rate at near SLS conditions [STE99].

Theoretical models of the sintering rate typically describe the viscous flow as the driving force for the sintering of polymers [GER96]. New experiments, however, show insufficient consistency between the viscous theory and experimental data. The main reason is the assumption that polymers have purely viscous properties. In reality, the rheological properties of polymers are viscoelastic and can only be described as being viscous for long time scales [FER80]. In this paper, the viscous theory of Pokluda ([4], [5]) is expanded by the viscoelastic behavior of polymers. Therefore, the viscous description of the tension in [4] is replaced by a viscoelastic description [FER80] ([6]-[10]):

$$\frac{dW_v}{dt} = P_v = \eta_0 \bar{v} : \left( \bar{v} + \bar{v}^T \right) dV, \quad [4]$$

$$\frac{d\theta}{dt} = \frac{\sigma}{\eta_0 a_0} \frac{2^{-\frac{5}{3}} \cos(\theta) \sin(\theta) (2 - \cos(\theta))^{\frac{1}{3}}}{(1 - \cos(\theta)) (1 + \cos(\theta))^{\frac{1}{3}}}$$

$$\theta(0) = \theta_0 = 0 \quad [5]$$

$$\vec{\sigma}_s(t) = \int_0^t G(t-t) \dot{\vec{\epsilon}} dt, \quad [6]$$

$$\vec{\epsilon}(t) = \int_0^t J(t-t) \dot{\vec{\sigma}}_s dt, \quad [7]$$

$$G(t) = G_e + \sum_{i=1}^n G_i e^{-\frac{t}{\tau_i}}, \quad [8]$$

$$J(t) = J_g + \sum_{i=1}^n J_i \left(1 - e^{-\frac{t}{\tau_i}}\right) + \frac{t}{\eta_0}. \quad [9]$$

where  $\sigma$  is the surface tension,  $\eta$  is the viscosity and  $x$  is the radius of the sintering neck,  $P_v$  is the power dissipation,  $v$  is the velocity tensor,  $\theta$  the sintering angle  $G(t)$  the relaxation modulus and  $J(t)$  the creep compliance.

The viscous description of the tension in [4] is replaced by the viscoelastic description of [6].

$$P_v = \int_v \sigma_s(t) \vec{v}(t) dV. \quad [10]$$

Hence, the viscoelastic sintering theory can be formulated as follows:

$$\int_0^t G(t-t) \frac{2 \sin[\theta(t)]}{[1 + \cos[\theta(t)]] [2 - \cos[\theta(t)]]} \frac{d}{dt} \theta(t) dt = \frac{F(\theta(t))}{P(\theta(t))},$$

$$F(\theta(t)) = \sigma \frac{8 \pi a_0^3 2^{\frac{1}{3}} \cos(\theta(t)) \sin(\theta(t))}{[1 + \cos(\theta(t))]^{\frac{1}{3}} [2 - \cos(\theta(t))]^{\frac{5}{3}}}, \quad [11]$$

$$P(\theta(t)) = \frac{2 \sin[\theta(t)]}{[1 + \cos[\theta(t)]] [2 - \cos[\theta(t)]]} 8 \pi a_0^3.$$

The relaxation modulus  $G(t)$  is determined by comparing [8] with experimental data from rheometer measurements. The validity of the viscoelastic sintering theory is controlled by a sintering experiment at near SLS condition [STE99]: powder is placed on a heating stage and preheated to the desired temperature. The powder is then exposed to CO<sub>2</sub> laser radiation (Synrad laser, 10W). An optical sensor (Jurca Optoelektronik) is used to follow the change of the sample height  $dh$ . Since a temperature gradient exists in the heated spot, it follows that only an average change in solid fraction can be measured. In order that the model could be properly evaluated, the experiment was simulated under consideration of the temperature distribution. *Figure 5* indicates, in comparison to the viscous theory of Pokluda, good

consistency of the new viscoelastic sintering theory and the experimental data. The absolute change in height as well as the dynamics of the sintering process are described properly.

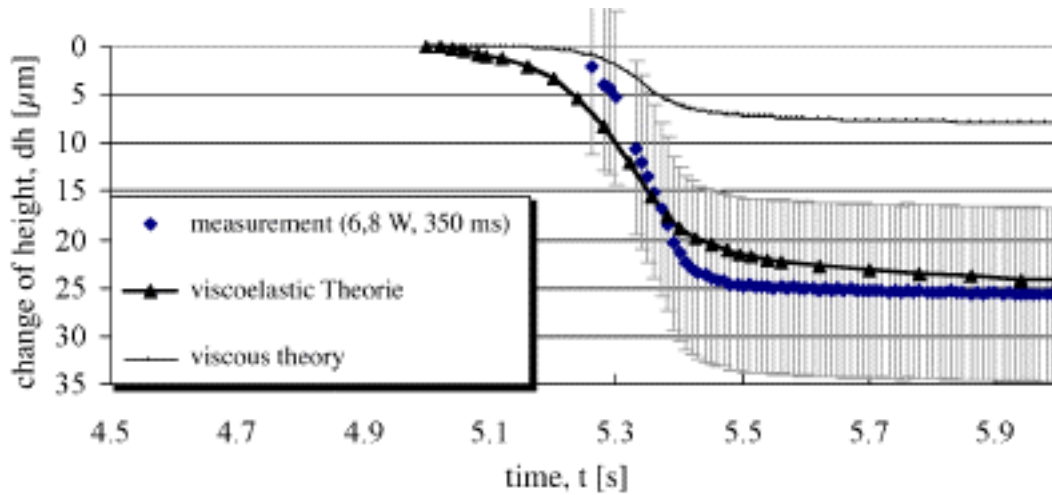


Figure 5: comparison of viscoelastic sintering theory and experimental data

### Simulation

Finally, the different physical processes are implemented into an FEM simulation. To enable verification of the process simulation, the sintering dynamics experiment has been simulated. The measured surface temperature (/STE99/) was compared with the calculated surface temperature in the laser spot. Figure 6 indicates the excellent correspondence of process simulation and physical reality.

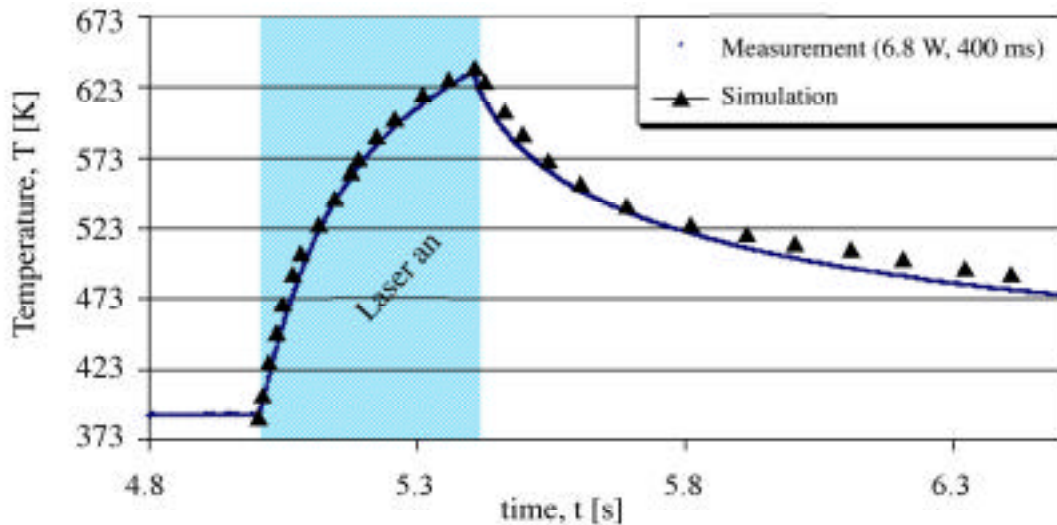
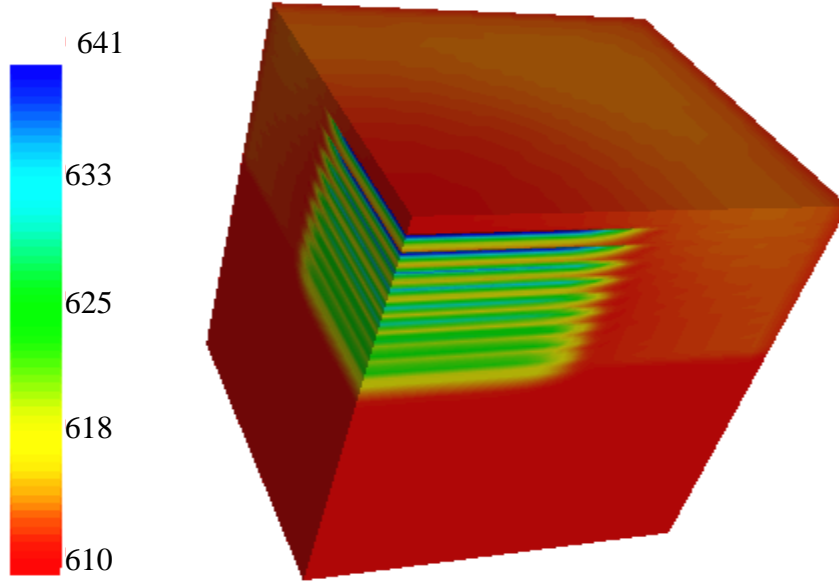


Figure 6: Simulated and measured surface temperature in the laser spot

Currently, the simulation is used to describe the generative build-up of simple geometries. This permits the analysis of major problems incurred in the SLS process. Figure 7 depicts the rising sintering density with a corresponding increase in the number of layers. Moreover, the dependence of the sintering density on the scanning vector was confirmed and quantified. As experimentally analyzed (/NÖK97/), the sintering density decreases with the rising length of

the scan vector. In addition, the density distribution of a layer exposed alongside is analyzed in *Figure 8*. Due to the cold environment, the heat in the primary exposed lines ( $y = 0$ ) can dissipate much better than in the lines exposed later. Hence, the resulting sintering density is much lower.

**Density,  $\rho$  [g/cm<sup>3</sup>]**



*Figure 7: Change of density with a rising number of layers*

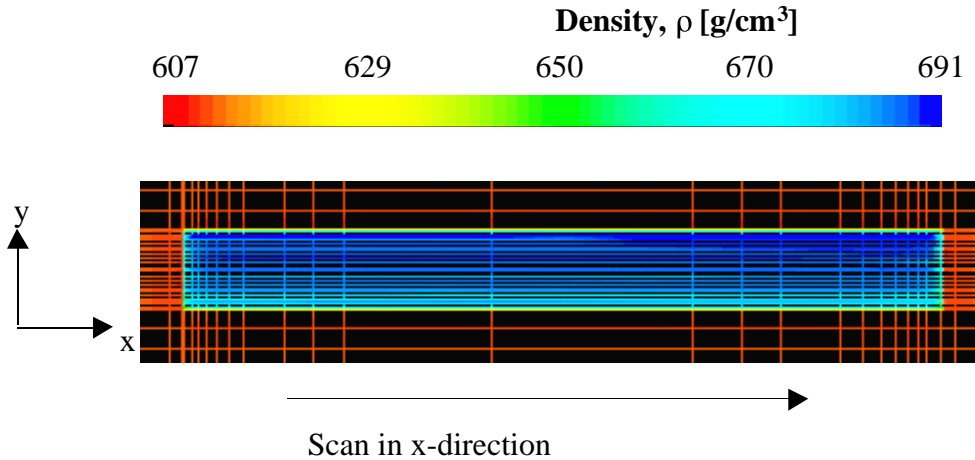


*Figure 8: Density distribution in a layer exposed alongside*

## Conclusion

On the basis of the detailed and SLS-relevant description of the simple physical processes, an FEM simulation is provided. This simulation considers the interaction of the simple processes and can, therefore, determine its influence on the SLS process. In addition, this simulation is used for a discussion of the most critical problems incurred in Selective Laser Sintering. At present, the simulation is deployed to develop and estimate geometry-independent scanning strategies. Moreover, the complete thermal economy of the machine is analyzed and optimized. The current interest of research is focused on the reduction of data. Once the



amount of data can be handled, the simulation will be used to calculate 3D-shrinkage problems, optimize geometry-dependent scan strategies and control both the laser power and the complete heating system, thus providing a tool for the systematic optimization of the SLS process.

## Acknowledgement

The authors kindly thank Dr. Neal K. Vail for his input on this work.

## References

<b>C. T. Bellehumeur /BEL98/:</b> <i>The role of viscoelasticity in polymer sintering</i> Rheol Acta 37: 270 – 278 (1998)	<b>S. Nöken /NÖK97/:</b> <i>Technologie des Selektiven Lasersinterns von Thermoplasten, Diss</i> Shaker Verlag, Band 8, 1997
<b>J. D. Eshelby /ESH49/:</b> <i>Seminar on the kinetics of sintering</i> Metals transaction 185 (1949), S 806 – 807	<b>J. I. Peltoniemi /PEL93/:</b> <i>Light Scattering in Planetary Regoliths and Cloudy Atmospheres</i> Academic dissertation, Helsinki (1993)
<b>J. D. Ferry /FER80/:</b> <i>Viscoelastic properties of polymers</i> John Wiley & Sons, New York (1980)	<b>O. Pokluda /POK97/:</b> <i>Modification of Frenkel's model for sintering</i> AIChE Journal, Dec97, Vol. 43, No. 12
<b>J. Frenkel /FRE45/:</b> <i>Viscous flow of crystalline bodies under the action of surface tension</i> <i>Journal of Physics, 1945, Vol IX, No. 5</i>	<b>E. U. Schlünder /SCH88/:</b> <i>Wärmeübertragung in Festbetten, Schüttgütern und Wirbelschichten</i> Georg Thieme Verlag Stuttgart, 1988
<b>R. M. German /GER96/:</b> <i>Sintering theory and practice</i> John Wiley & Sons, Inc. New York 1996	<b>M. Sun /SUN91/:</b> <i>A Model for Partial Viscous Sintering</i> Solid Freeform Fabrication Symposium 1991
<b>A. Ishimura /ISH78/:</b> <i>Wave Propagation and Scattering in Random Media, Vol. 1: Single Scattering and Transport Theory</i> Academic Press, New York (1978)	<b>J. Steinberger, K Manetsberger, J. Shen, J. Müllers:</b> <i>Measuring the Sintering Dynamics of Polymeric Powders at near SLS-Conditions</i> Solid Freeform Fabrication Symposium, Proceedings (1999)
<b>A. Kokhanovsky /KOK99/:</b> <i>Optics of light scattering media, Problems and Solutions</i> Wiley-Praxis, Chichester (1999)	<b>C. L. Tien /TIE87/:</b> <i>Thermal Radiation in Particulate Media with Dependent and Independent Scattering</i> Annual Review of Numerical Fluid Mechanics and Heat Transfer, 1, pp. 1-32, 1987
<b>J. C. Nelson /NEL93/:</b> <i>Selective Laser Sintering: A Definition of the Process and Empirical Sintering Model</i> ; PhD, Dissertation , 1993; Univ. of Texas	